Geologic and Topographic Features of Slope Failure Sites in the Aso Caldera Wall Induced by the 2016 Kumamoto Earthquake

Haruka SAITOU[1,*], Shin'ya KATSURA[2], Ryota UMETANI[1], Mio KASAI[2] and Tomomi MARUTANI[2]

[1] Graduate school of Agriculture, Hokkaido University (Kita 8, Nishi 5, Kita-ku, Sapporo, Hokkaido 060-0808, Japan)
[2] Research Faculty of Agriculture, Hokkaido University (Kita 8, Nishi 5, Kita-ku, Sapporo, Hokkaido 060-0808, Japan)
*Corresponding author. E-mail: saitoudaifuku@eis.hokudai.ac.jp

Large-scale earthquakes can trigger slope failures. To effectively implement countermeasures to mitigate damage caused by slope failures, it is necessary to identify locations where the risk of slope failure is high. The geologic and topographic features of slope failure in the Aso Caldera wall induced by the 2016 Kumamoto earthquake were examined as a case study. The geology was roughly divided into three categories: pyroclastic flow deposits, andesite, and talus accumulation. The elevation, slope, and curvature were calculated using geographic information system (GIS) software and a digital elevation model (DEM) obtained before the earthquake; these parameters were then used as topographic indices. The analysis results showed that slope failures occurred most densely in the pyroclastic flow deposits. Within this geology, slope failure frequency increased proportionally with slope, and more slope failures occurred at sites with a positive curvature (i.e., convex slopes). There was no relationship between elevation and slope failure. We conclude that sites with these geologic and topographic features are prone to slope failure induced by large-scale earthquakes.

Key words: 2016 Kumamoto earthquake, geology, GIS, slope failure, topography

1. INTORODUCTION

A series of earthquakes with epicenters mainly in Kumamoto Prefecture, Kyushu Region, Japan, occurred in April 2016. The main shock of the 2016 Kumamoto earthquake on April 16 had a maximum seismic intensity of 7 on the Japan Meteorological Agency (JMA) 7-stage seismic scale and a JMA magnitude of 7.3. The Aso Caldera is a large caldera in Kumamoto Prefecture that was formed by catastrophic eruptions 270,000–90,000 years ago, and which measures about 17 km in the east–west direction and about 25 km from north to south. A JMA seismic intensity of 6 lower occurred in the Aso Caldera wall, which resulted in numerous slope failures and extensive damage (**Fig. 1**).

Several studies have been conducted of the geologic and topographic features of sites that

Fig.1 Photographs of slope failures in the Aso Caldera wall (taken by the authors, December 19–20, 2017)

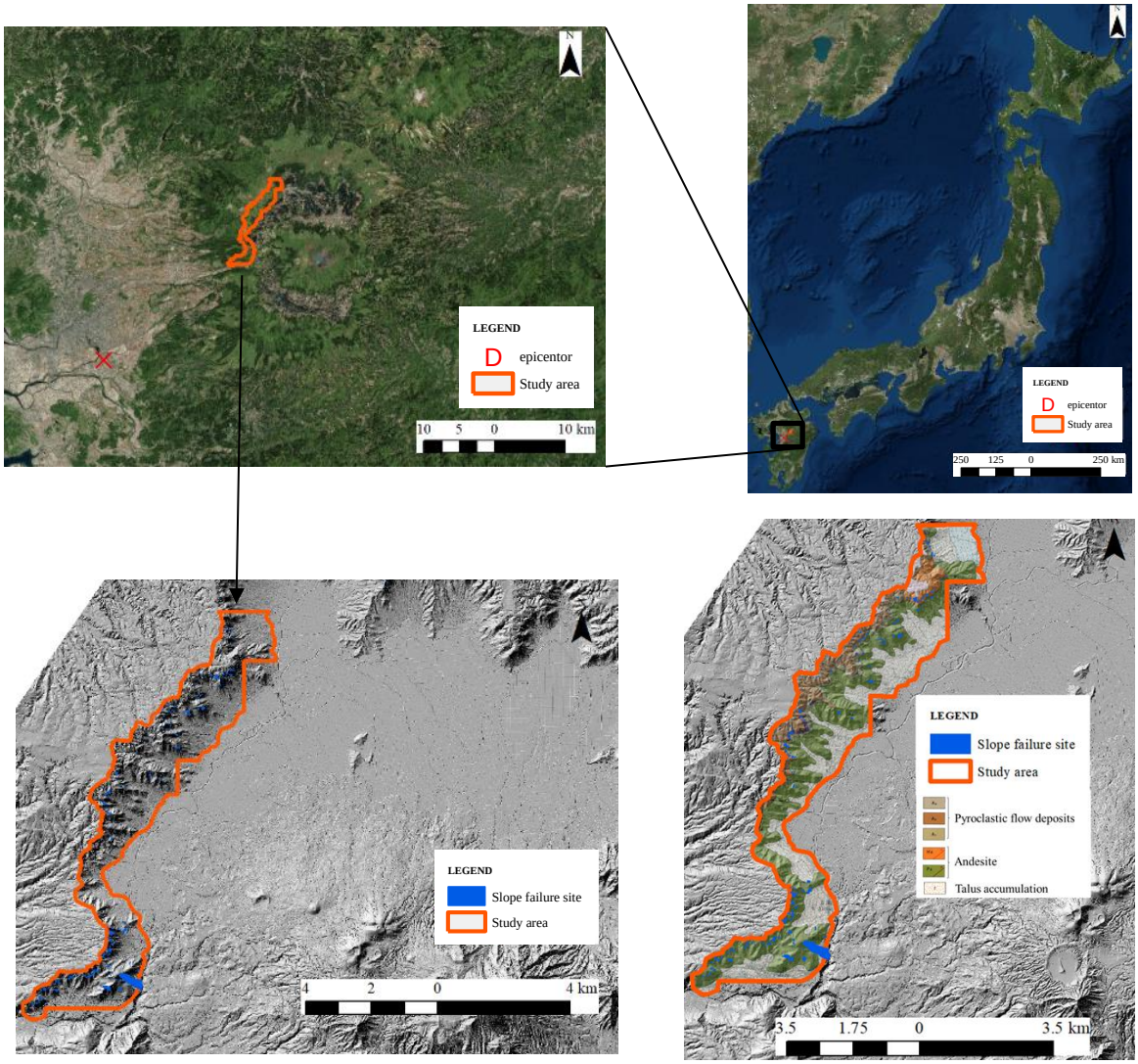

Fig.2 Study area (drawn based on the map provided by the Geospatial Information Authority of Japan)

including the 1995 Southern Hyogo Prefecture Earthquake [*Kawabe et al.*, 1997], the 1997 northwestern Kagoshima earthquake [*Jitousono et al.*, 1998], and the Kamishiro fault earthquake in Nagano Prefecture [*Katsura et al.*, 2016]. However, cases of slope failure due to earthquake remain greatly outnumbered by slope failure due to rainfall. To effectively implement countermeasures to mitigate damage caused by earthquake-induced slope failures, it is necessary to identify locations where the risk of slope failure is high. The purpose of this study was to clarify the geologic and topographic features of sites in the Aso Caldera wall where slope failure was caused by the 2016 Kumamoto earthquake.

2. EARTHQUAKE SUMMARY

According to the JMA, the main shock of the 2016 Kumamoto earthquake had a magnitude of 7.3 (seismic center: 32°45.3’N, 130°45.8’E; 12 km depth) on April 16 at 01:25, 2016. This right strike-slip fault earthquake had a tensile axis in the north–south direction [*Japan Meteorological Agency*, 2016]. The earthquake caused numerous landslides and 190 sediment-related disasters in Kyushu Region [*Ministry of Land, Infrastructure, Transports and Tourism*, 2018], killing 10 people and causing the complete destruction of 22 houses and severe damage to a further 13 houses.

3. METHOD

3.1 SUTUDY AREA

The study area was the northwestern part of the Aso Caldera wall, Kumamoto Prefecture, Japan (20.7 km^2; **Fig. 2**). The geology of the Aso Caldera wall consists of pyroclastic flow deposits, including welted tuff formed by catastrophic eruptions about 270,000–90,000 years ago (Aso-1 to 4), andesite older than Aso-1 to 4, and talus accumulations (formed by rock debris accumulation), roughly from the top to the bottom. The area and average slope of each geologic feature are shown in **Table 1**.

3.2 DATA COLLECTION

3.2.1 SLOPE FAILURE SITES

In the study area, light detection and ranging (LiDAR) data were obtained for 2012 (before the earthquake) and 2016 (after the earthquake). A digital elevation model (DEM) created from the LiDAR data before and after the earthquake was converted to create raster data. Using geographic information system (GIS) software, we outlined an area where the elevation showed a negative change from before to after the earthquake, and defined this area as the slope failure site. We confirmed the locations of slope failure by comparison with aerial photographs taken by the Geospatial Information Authority of Japan (GSI) immediately after the earthquake (April 16–20, 2016). As a result of this analysis, we identified 184 slope failure sites.

3.2.2 GEOLOGY AND TOPOGRAPHY

We used the geology and elevation, slope, and curvature of the sites as topographic indices because these factors are frequently cited as influential factors in studies of earthquake-induced slope failure.

Slope and the curvature were calculated from the DEM before the earthquake using GIS. Curvature is an index representing the unevenness of the terrain; positive and negative values indicate convex and concave shapes, respectively. Both slope and curvature are calculated using the elevation of the target cell and that of the surrounding eight cells. For example, for a DEM with a 10-m cell size, these topographic indices represent a slope shape in the range of 30 m × 30 m (i.e., 900 m^2). To determine the appropriate cell size for the DEM, we investigated the area of each slope failure site (histogram, **Fig. 3**). We classified these areas into cell sizes of 5 (i.e., 225 m^2), 10 (900 m^2), and 15 m (2,025 m^2); 60% of the slope failure sites had an area between 225 and 2,025 m^2, and we determined that a 10-m DEM cell size was appropriate for this study.

The geology of the slope failure sites was identified based on a geological map of the Aso volcano [*Ono and Watanabe*, 1985]. As described above, we roughly classified the geology into three categories: Aso-1 to 4 pyroclastic flow deposits (including welted tuff), andesite older than Aso-1 to 4, and talus accumulation.

3.3 ANALYSIS OF SLOPE FAILURE SITE FEATURES

Table 1 Area, average slope, the number of slope failure, and the slope failure density for each geology

Geology	Area (km^2)	Average slope (°)	Number of slope failure	Slope failure density (/km^2)
Pyroclastic flow deposits	3.2	31.4	59	18.4
Andesite	10.1	31.3	121	12.0
Talus accumulation	7.4	14.5	4	0.5
Total/Average	20.7 (total)	24.4 (average)	184 (total)	8.9 (average)

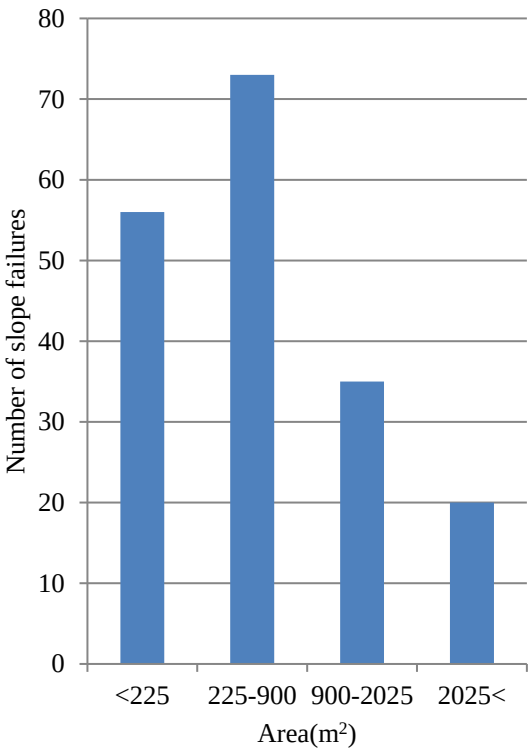

Fig.3 Area of slope failure sites

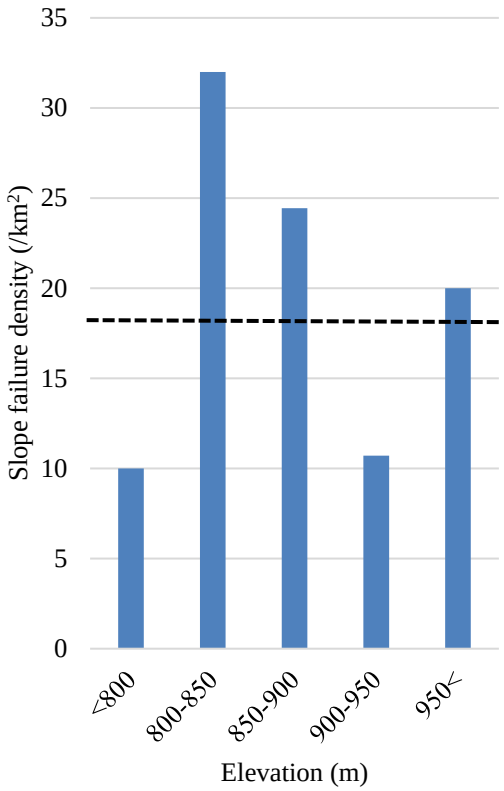

Fig.4 Slope failure density for each elevation class within the pyroclastic flow deposits

Topographic indices for each slope failure site were calculated by averaging the values of all cells overlapping all or part of the polygon representing the slope failure site. The geology of each site was determined by superposing its polygon on the geological map using GIS. When a polygon overlapped more than one geology class, we adopted the geology class that covered the highest elevation within the site. Slope failure density (the number of slope failures per unit area) was used to evaluate the risk, rather than the number, of slope failures, because the area of each class within each factor was different.

4. RESULTS AND DISCUSSION

4.1 GEOLOGY

The slope failure density for each geology class is shown in **Table 1**. The slope failure density of pyroclastic flow deposits (18.4/km^2) and andesite (12.0/km^2) exceeded the average slope failure density for the whole study area (8.9/km^2), suggesting that pyroclastic flow deposits and andesite are more prone to slope failure than talus accumulation, likely because the average slope among the pyroclastic flow deposit and andesite classes was larger than that of the talus accumulation class (**Table 1**); moreover, as will be described later, slope failure tends to occur at locations with larger slopes. The slope failure density of the pyroclastic flow deposits was larger than that for andesite, probably because the pyroclastic flow deposits were formed more recently and the degree of consolidation was small.

Therefore, we focused on pyroclastic flow deposits in the following sections.

4.2 ELEVATION

The slope failure density for each elevation class is shown in **Fig. 4**. The average slope failure density in the pyroclastic flow deposits (18.4/km^2) is indicated by a broken line. In the 800–900 m and > 950 m classes, slope failure density was larger than 18.4/km^2, indicating that slope failure occurred more frequently at these elevation ranges. Although some previous studies [e.g., *Jitousono et al.*, 1998] have suggested that slope failure density increases with increasing elevation, probably due to the amplification of seismic waves at high

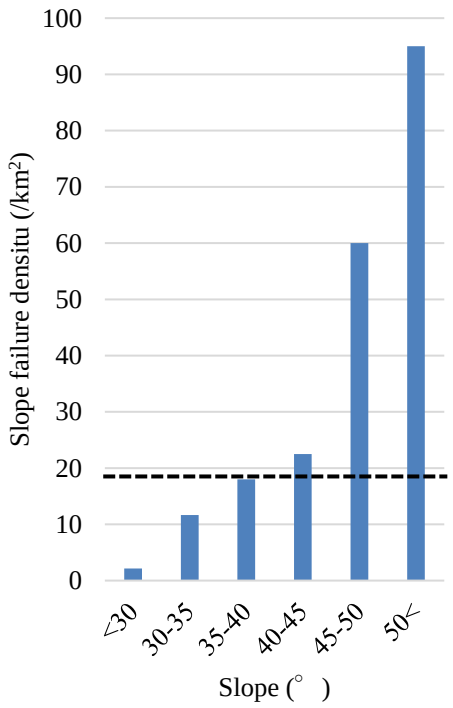

Fig.5 Slope failure density for each slope class within the pyroclastic flow deposits

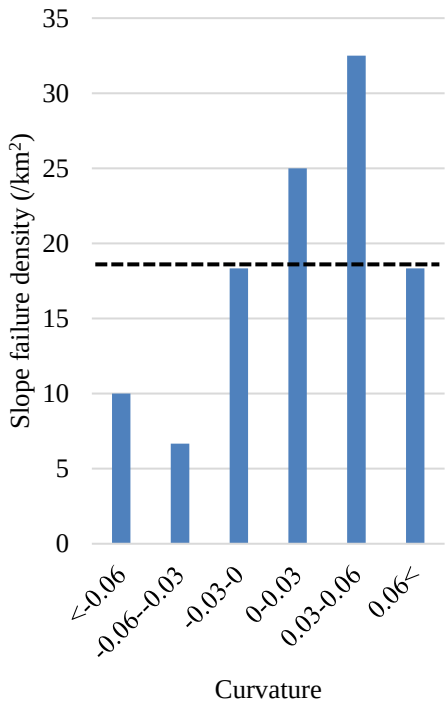

Fig.6 Slope failure density for each curvature class within the pyroclastic flow deposits

elevation [*Yamaguchi and Kawabe*, 1982], the current study detected no such tendency. We concluded that there was no relationship between elevation and slope failure.

4.3 SLOPE

The slope failure density for each slope class is shown in **Fig. 5**. Slope failure density clearly increased with increasing slope, and the average slope failure density (18.4/km^2) was exceeded in slope classes > 40°. Therefore, slope was found to influence slope failure, with steeper slopes being more prone to failure, probably because downward force on an inclined soil mass increases as slope increases, as has been reported in many previous studies [e.g., *Okimura et al.*, 1997].

4.4 CURVATURE

The slope failure density for each curvature class is shown in **Fig. 6**, which demonstrates that the average slope failure density was exceeded for curvatures between 0 and 0.06. This finding suggests that a convex slope is more prone to slope failure, likely because seismic waves are amplified at convex slopes [*Yasuda et al.*, 2006; *Nishida et al.*, 1997].

5. SUMMARY

In this study, we analyzed the geologic and topographic features of the Aso Caldera wall at sites that had experienced slope failure caused by the main shock of the 2016 Kumamoto earthquake, which occurred on April 16, 2016. Our findings are summarized as follows.

1) Pyroclastic flow deposits are more prone to slope failure than andesite and talus accumulation, probably due to their steeper slopes and recent age of formation.

2) There was no relationship between elevation and slope failure.

3) Slope failure was more likely to occur with increasing slope, especially at slopes > 40°.

4) Convex slopes were more prone to slope failure than concave slopes, probably due to the amplification of seismic waves.

In this study, we clarified the geologic and topographic features of the slope failure sites caused by the 2016 Kumamoto earthquake in the Aso Caldera wall. In future work, we recommend

the further development of these methods of evaluating slope failure risk induced by a large-scale earthquake, to include risk assessment for individual slopes.

ACKNOWLEDGMENTS: This research was conducted under the subject “Occurrence and flow of mountain slope failure with driftwood in volcanic regions” and “Mechanisms of and countermeasures against chain and complex sediment-related disasters caused by large earthquakes and accompanying ground deterioration” by the river and sabo technology open research and development system of the Ministry of Land, Infrastructure Transport and Tourism (MLIT). The LiDAR data used in this study were provided by the Kyushu Regional Development Bureau, MLIT.

REFERENCES

Japan Meteorological Agency (2016): The 2016 Kumamoto Earthquake, http://www.data.jma.go.jp/svd/eqev/data/2016_04_14_kumamoto/index.html#kumamoto_data. Reference date: November 30, 2017 (in Japanese).

Jitousono, T., Shimokawa, E., Matsumoto, M. and Teramoto, Y. (1998): Distribution and topographical characteristics of slope failures caused by earthquake in Northwestern part of Kagoshima in 1997, Journal of the Japan Society of Erosion Control Engineering, Vol. 51, No. 1, pp. 38–45 (in Japanese with English abstract).

Katsura, S., Kimura, T., Maruyama, K. and Ishida, K. (2016): Characteristics of landslides induced by the Kamishiro Fault Earthquake in Nagano Prefecture on November 22, 2014, Journal of the Japan Landslide Society, Vol. 53, No. 3, pp. 11–20 (in Japanese).

Kawabe, H., Tsujimoto, F. and Hayashi, S. (1997): The distribution of slope collapses in the Rokko Mountains caused by the 1995 Hyogo-ken Nanbu Earthquake, Journal of the Japan Society of Erosion Control Engineering, Vol. 49, No. 5, pp. 12–19 (in Japanese with English abstract).

Ministry of Land, Infrastructure, Transports and Tourism (2018): Occurrence of sediment-related disasters in 2016,http://www.mlit.go.jp/river/sabo/jirei/h28dosha/H28dosyasaigai.pdf. Reference date: May 7, 2018 (in Japanese).

Nishida, K., Kobayashi, S. and Mizuyama, T. (1997): DTM based topographical analysis of landslide caused by an earthquake, Journal of the Japan Society of Erosion Control Engineering, Vol. 49, No. 6, pp. 9–16 (in Japanese with English abstract).

Okimura, T., Yoshida, N., Okunishi, K. and Torii, N. (1997): A consideration of the mechanism of slope failure in the Rokko mountain range caused by the 1995 Southern Hyogo Prefecture Earthquake, Disaster Prevention Research Institute Annuals, Kyoto University, No. 40B-1, pp. 115–125 (in Japanese; the title is a tentative translation by the authors from the original).

Ono, K. and Watanabe, K. (1985): Geological map of Aso Volcano (1:50,000) (in Japanese).

Yamaguchi, I. and Kawabe, H. (1982): Study of characteristics of disaster at mountainous district due to earthquake, Shin-Sabo, Vol. 35, No. 2, pp. 3–15 (in Japanese with English abstract).

Yasuda, Y., Tsuchiya, S., Mizuyama, T., Matsumura, K., Ochiai, H., Takahashi, M. and Tang, W. (2006): Topographic effects of the seismic slope displacement and ground acceleration by earthquake using a dynamic response analysis, Journal of the Japan Society of Erosion Control Engineering, Vol. 59, No. 4, pp. 3–11 (in Japanese with English abstract).